Supporting Information

Electroless Nanoparticle Film Deposition Compatible with Photolithography, Microcontact Printing, and Dip-pen Nanolithography Patterning Technologies

Lon A. Porter, Jr., Hee Cheul Choi, J. M. Schmeltzer, Alexander E. Ribbe, Lindsay C. C. Elliott, and Jillian M. Buriak*

[*] Prof. Dr. Jillian M. Buriak, Lon A. Porter, Jr., Hee Cheul Choi, J. M. Schmeltzer, Lindsay C. C. Elliott, and Dr. Alexander E. Ribbe
Department of Chemistry, 1393 Brown Laboratories, Purdue University, West Lafayette, IN 47907-1393
Fax: (+1) 765-494-5302
E-mail: buriak@purdue.edu

Experimental Supplement with Additional Characterization

Materials. The following reagents were purchased from the indicated suppliers and used without modification: n-type (Sb-doped, 7 – 23 Ω·cm) and p-type (Ga-doped, 0.004 - 0.020 Ω·cm) crystalline germanium wafers (Waferworld, (100) orientation), copper (Aldrich, foil), zinc (Aldrich, foil, 0.127 mm thick, 99.9%), tin (Aldrich, foil, 0.127mm thick, 99.9%), hydrofluoric acid (Mallinckrodt, 48%), H_2O_2 (Mallinckrodt, 30%), 1-dodecene (Aldrich, 98%), acetonitrile (Aldrich, 99.8%), $HAuCl_4{\cdot}3H_2O$ (99.9%, Aldrich), $Na_2PdCl_4{\cdot}3H_2O$ (Pd, 99%, Strem), $Na_2PtCl_4{\cdot}xH_2O$ (%Pt 42.65, Strem). Absolute ethanol was purchased from Pharmco Products Inc. Distilled water (18 MΩ) was purified using a Millipore (Barnstead) system. Optima grade methylene chloride and tetrahydrofuran (THF) were purchased from Fisher and purified utilizing a Grubbs/Dow Chemical solvent purification apparatus. All other solvents and materials were obtained from commercial sources and used without modification.

Instrumentation

Scanning Electron Microscopy (SEM) and Energy Dispersive Spectroscopy (EDS). In order to perform structural and qualitative analysis, SEM and EDS were employed with a JEOL JSM-35 CF.

X-Ray Photoelectron Spectroscopy (XPS). XPS spectra were measured using an Axis Ultra spectrometer (Kratos Analytical) with a monochromatic Al Kα source (225 W power). Survey (low-resolution) spectra were accumulated at a pass energy of 160 eV and were averaged from two scans with a step of 1000 meV. Adventitious hydrocarbon deposits from handling in air were used to reference all spectra at 284.0 eV.**General Procedure for Electroless Formation of Precious Metal Nanoparticles (Utilized for**

SEM, EDS, and XPS Experiments). Aqueous $AuCl_4^-$, $PdCl_4^{2-}$, and $PtCl_4^{2-}$ 'ink' solutions were prepared by dissolving $HAuCl_4{\cdot}3H_2O$, $Na_2PdCl_4{\cdot}3H_2O$, $Na_2PtCl_4{\cdot}xH_2O$, into deionized water (18 MΩ·cm), respectively. The 'paper' substrates, Ge, Cu, Al, Zr, Zn, and Sn, were degreased by rinsing with dichloromethane, THF, and pentane. Metal foils were subsequently immersed into a 1:1 0.1 M HCl: 0.05 M H_2SO_4 solution and then rinsed with copious amounts of deionized water prior to use. Each substrate was cut into 0.5 cm × 0.5 cm rectangles and soaked in scintillation vials containing the aqueous 'ink' for the designated time at room temperature.

XPS Data for Nanoparticle Films

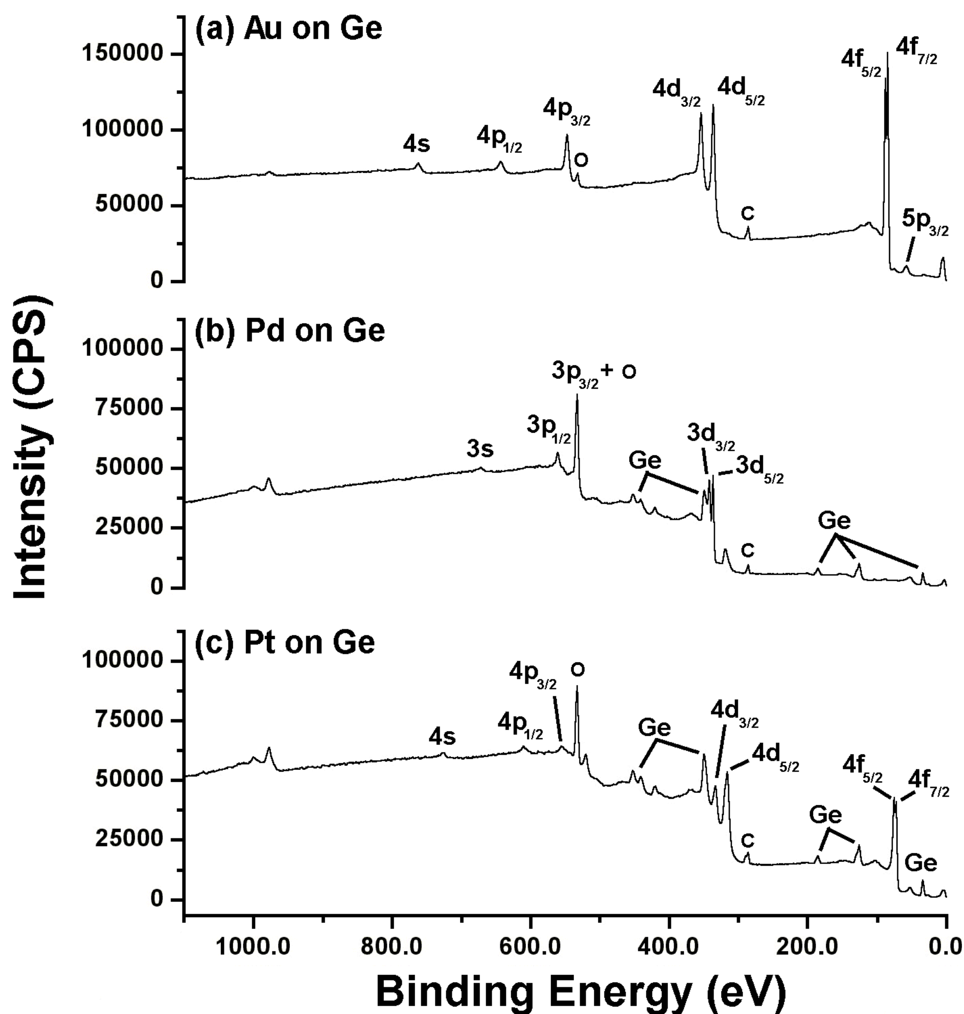

Figure SI-1. XPS of (a) Au, (b) Pd, and (c) Pt nanoparticles deposited on Ge from 1 mM aqueous $HAuCl_4$, Na_2PdCl_4, and Na_2PtCl_4 after 60 min.

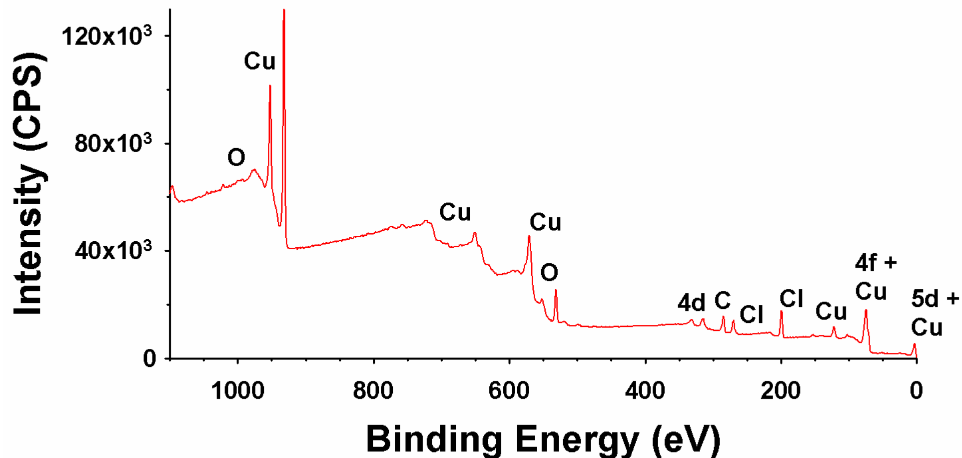

Figure SI-2. XPS of Pt nanoparticles deposited on Cu from 20 mM Na_2PtCl_4 after 3 min.

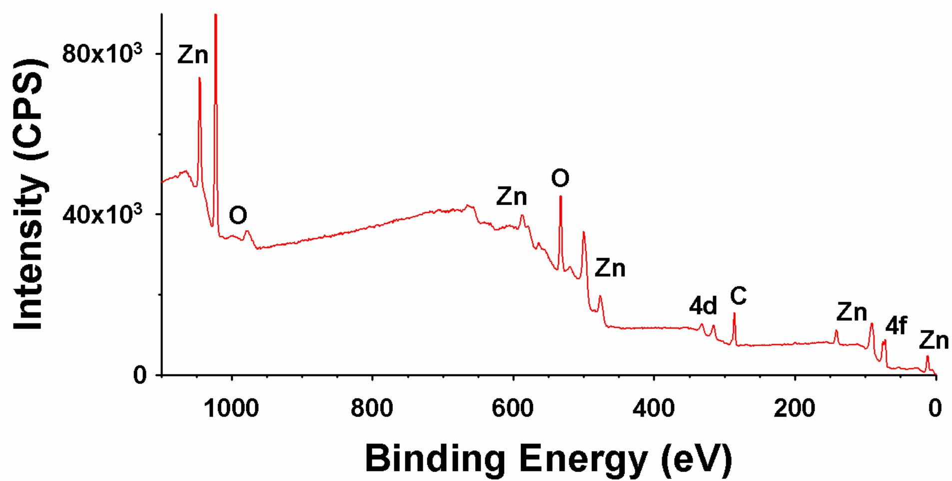

Figure SI-3. XPS of Pt nanoparticles deposited on Zn from 20 mM Na_2PtCl_4 for 3 min.

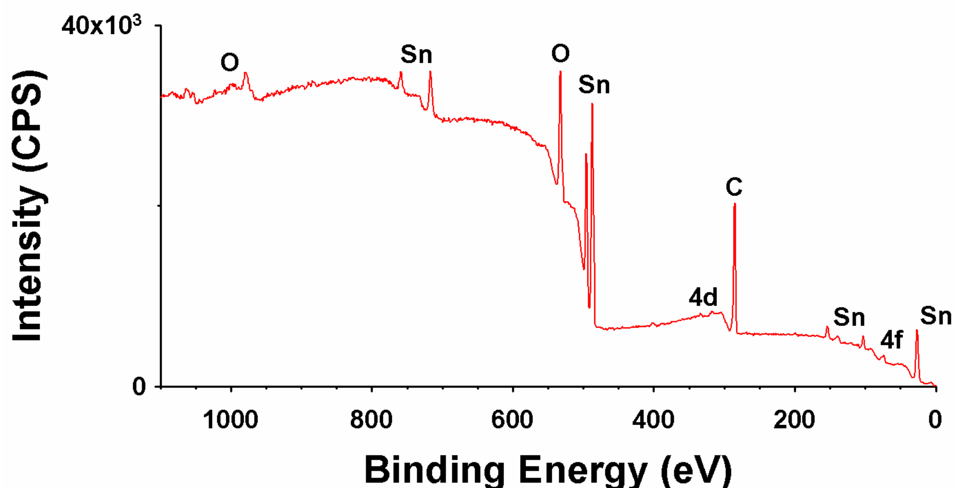

Figure SI-4. XPS of Pt nanoparticles deposited on Sn from 20 mM Na_2PtCl_4 for 3 min.

Patterning Procedures: (i) Photolithography

Hydride Termination. Hydride termination of the Ge wafers was accomplished with the following procedure: the Ge surfaces were soaked for 1 min in aqueous 30% H_2O_2, and rinsed thoroughly with 18 MΩ water. The wafer fragment was then immersed in an aqueous 10% HF solution for 10 min, and was finally rinsed with ethanol/pentane and blown dry with a stream of nitrogen.

Photopatterned UV Induced Hydrogermylation. A freshly prepared hydride-terminated Ge substrate was transferred to an inert atmosphere. Approximately 0.1 mL of 1-dodecene, filtered through alumina to remove peroxides, was dropped onto the Ge surface. A nickel "micromesh" grid (Internet, Inc., 10 μm feature size), serving as a photomask, was placed onto the Ge substrate. A brass washer was then employed to secure the photomask, and the surface was then exposed to a mercury vapor lamp with 254 nm radiation from either a UV handlamp (Fisher, 1100 $\mu W/cm^2$ at 25 cm), a Rayonet reactor (9 mW/cm^2 at 2 cm), or a penlight source (Jelight, 9 mW/cm^2 at 2 cm). UV photoinduced hydrogermylation was accomplished within 45 min and the sample subsequently washed with copious amounts of ethanol, pentane, and methylene chloride.

Deposition of Photopatterned Surfaces. After UV induced hydrogermylation or oxidation, the samples were immersed into aqueous solutions of either 2×10^{-3} M $HAuCl_4$, 2×10^{-3} M Na_2PdCl_4, or 2×10^{-2} M Na_2PtCl_4, depending on the metal species of interest. After soaking for 20-30 s, the substrates were removed from the metal solution and immediately washed with copious amounts of deionized water. The samples were finally blown dry utilizing a high-pressure stream of nitrogen.

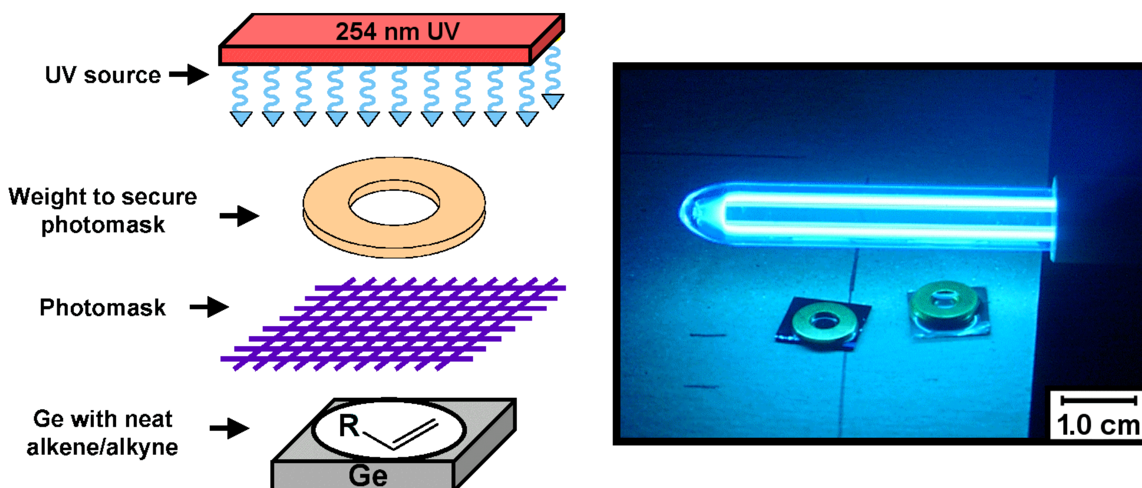

Figure SI-5. Photolithography setup: Approximately 0.1 mL of neat dodecene is applied to the surface of a hydride-terminated Ge(100) wafer (1 cm x 1 cm). A metal grid contact mask is held in contact with a small brass washer. Exposure is facilitated through the use of a 254 nm UV "penlight" source (Jelight, 9 mW/cm^2 at 2 cm). Hydrogermylation is completed at room temperature within 30 min, under an inert atmosphere. As expected, areas in close proximity to the washer edge (better mask contact) resulted in the best-resolved features. While crude, this apparatus provided for a lost-cost alternative to a contact mask aligner.

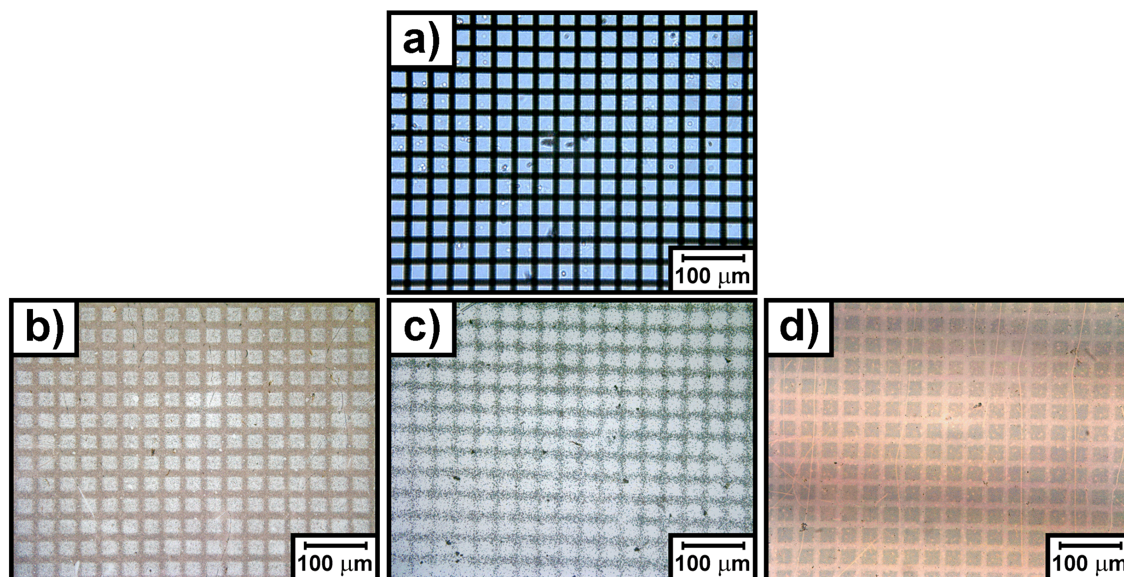

Figure SI-6. Optical micrographs of **a)** photomask and photopatterned deposition of **b)** palladium, **c)** platiunum, and **d)** gold on a Ge(100) surface. Selective hydrogermylation of 1-dodecene in the exposed areas results in decyl termination in the square regions; the grid lines remain hydride terminated. Exposure of the surface to an aqueous Na_2PtCl_4, $HAuCl_4$ (for gold deposition, reddish areas), or Na_2PtCl_4 (for platinum deposition, darker areas) solution results in selective deposition in the hydride terminated grid lines.

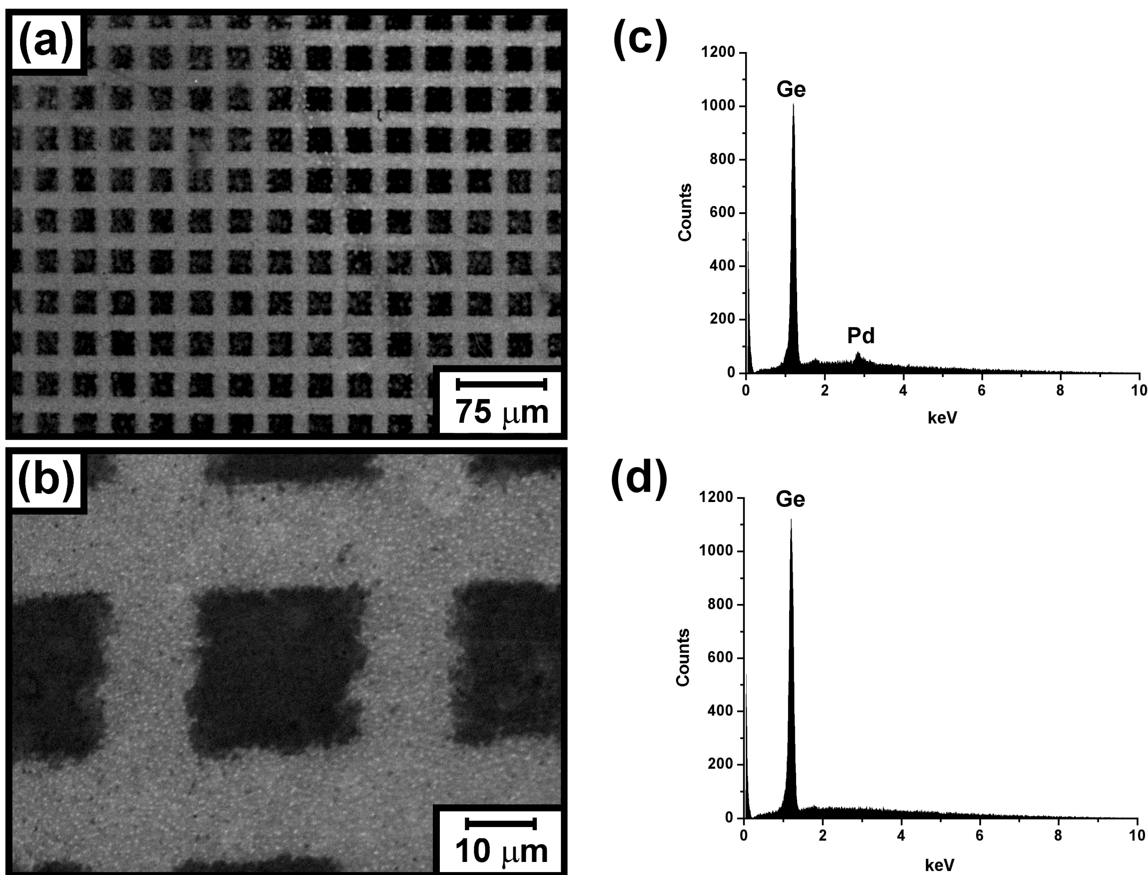

Figure SI-7. Scanning electron micrographs of photopatterned deposition of Pd upon a Ge(100) surface (a-b). Hydrogermylation of 1-dodecene by the Ge(100)-H_x surface, mediated by UV light in the unmasked areas results in dodecyl termination in the square regions; the grid lines remain hydride terminated. The organic monolayers acts as an effective ultrathin resist and immersion in aqueous 2 mM aqueous $PdCl_4^{2-}$ for 30 s results in selective deposition within the hydride-terminated grid lines. EDS confirms the deposition pattern, as observed by SEM. The EDS spectrum taken for the grid lines (c) confirms nanoparticles composed of Pd, whereas the Pd signal is absent from the EDS spectrum for the alkylated (square) regions (d).

Photopatterned UV Induced Oxidation. A brass washer was utilized to secure a nickel "micromesh" grid (Internet, Inc., 10 μm feature size) to the freshly prepared hydride-terminated Ge surface. The grid performed as a photomask and the surface was illuminated with a mercury vapor lamp supplying 254 nm radiation from either a Rayonet reactor (9 mW/cm^2 at 2 cm) or penlight source (Jelight, 9 mW/cm^2 at 2 cm). The illuminated regions undergo oxidation in air. Oxidation of the Ge surface exposed to UV radiation occurs in approximately 90 s. The Ge substrate was then removed and washed with ethanol and pentane. This leads to 5-25 μm-sized features of oxide and hydride. Immersion of the hydride/oxide surface into aqueous noble metal salt solutions results in a more rapid deposition of metal upon the germanium oxide regions, due to the difference in rates of the reduction. The germanium oxide dissolves in water, leading to intimate electrical contact between the semiconductor bulk and the metal salts and affording a

faster rate of deposition. In the case of silicon, however, this approach is not feasible since the native oxide has been shown to effectively prevent metal deposition due to its insolubility in water. The hydride surface oxidizes *in-situ* and subsequently dissolves in the aqueous medium. Metal salt reduction and deposition can then occur.

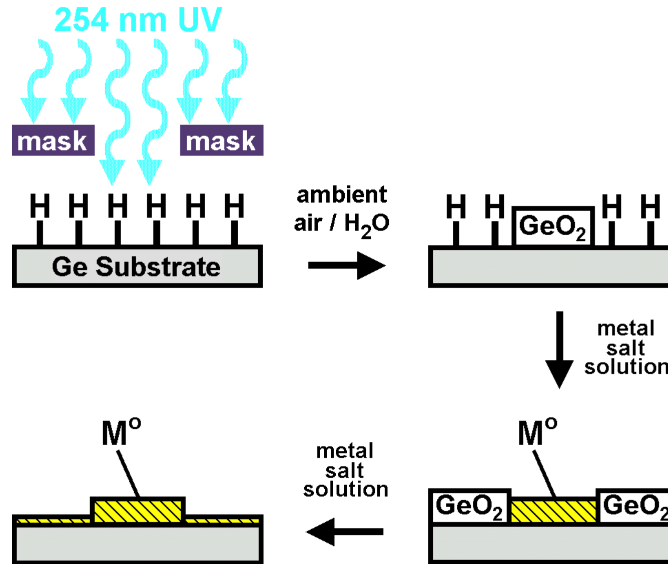

Figure SI-8. Outline of photopatterned UV induced oxidation approach. Using a metal grid contact mask, spatially defined areas of the hydride-terminated Ge(100) surface are photooxidized. Immersion of the hydride/oxide surface into a 2 mM Na_2PdCl_4 solution results in a more rapid deposition of metal upon the germanium oxide regions, due to the difference in rates of the reduction. The germanium oxide dissolves in water, leading to intimate electrical contact between the semiconductor bulk and the metal salts and affording a faster rate of deposition. The hydride surface oxidizes *in-situ* and subsequently dissolves in the aqueous medium. Metal salt reduction and deposition can then occur. Please note that layer thicknesses are not drawn to scale.

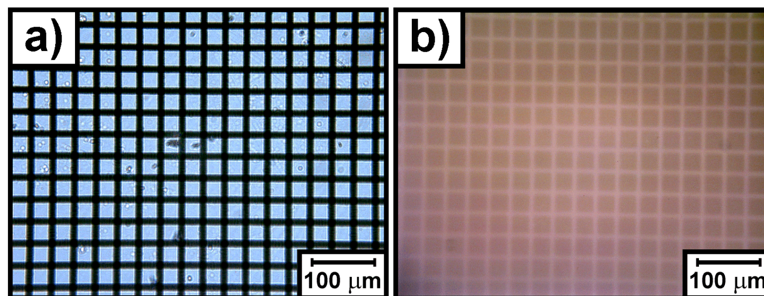

Figure SI-8. Optical micrographs of **a)** photomask and photopatterned deposition of **b)** palladium on a Ge(100) surface. Selective photooxidation in the exposed areas results in germanium oxide in the square regions; the grid lines remain hydride terminated. Exposure of the surface to a Na_2PdCl_4 solution results in a faster deposition rate for the oxidized square domains.

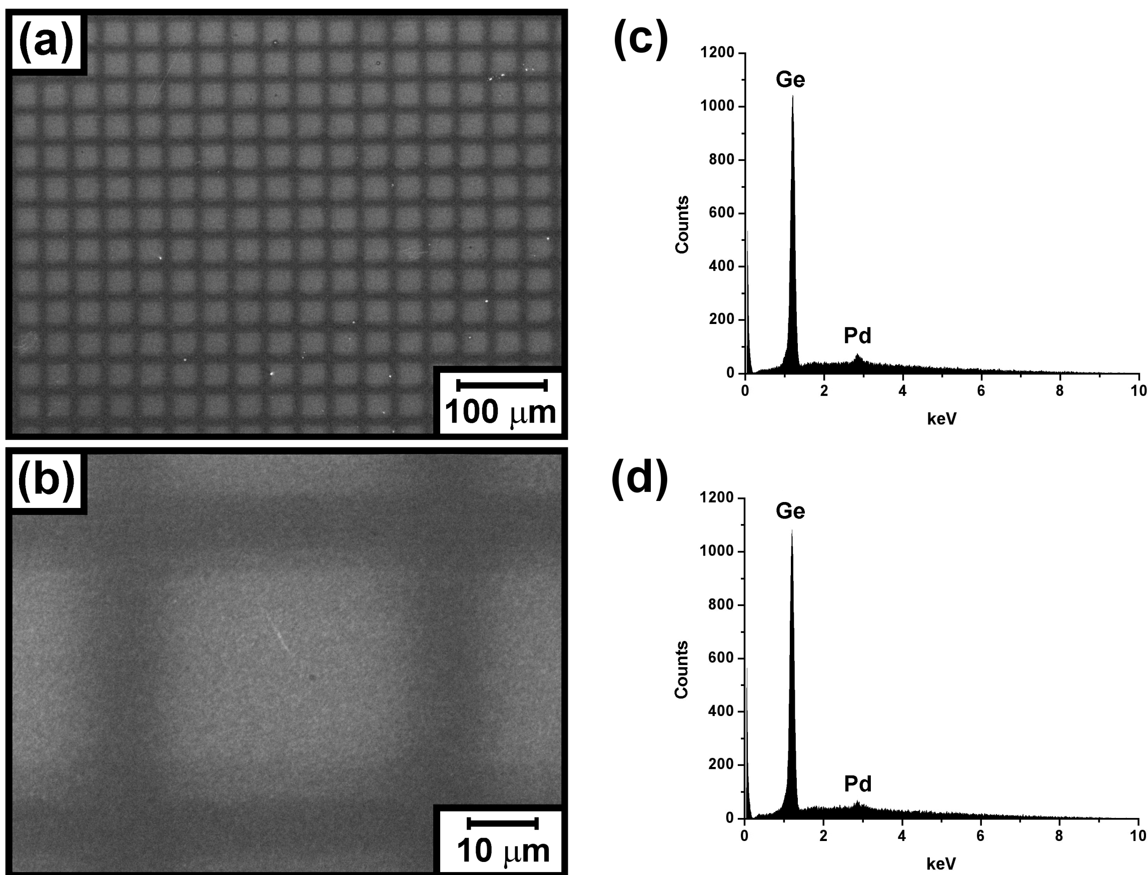

Figure SI-9. Scanning electron micrographs of photopatterned deposition of Pd upon a Ge(100) surface (a-b). Photooxidation of the hydride-terminated Ge(100)-H_x surface, mediated by UV light in the unmasked areas results in oxidized square regions; the grid lines remain hydride terminated. The germanium oxide dissolves in water, leading to intimate electrical contact between the semiconductor bulk and the metal salts and affording a faster rate of deposition. EDS confirms the deposition pattern, as observed by SEM. The EDS spectrum taken for the oxidized square domains (c) confirms nanoparticles composed of Pd, whereas the Pd signal is less intense in the EDS spectrum for the grid lines (d). This photolithographic method results in less selectivity of metal deposition as compared to the hydrogermylation method.

Patterning Procedures: (ii) μ-CP

Preparation of PDMS Stamps. The patterned poly(dimethylsiloxane) (PDMS) stamps were produced employing commercially available Sylgard 184 (Dow Corning). A 10:1 v/v mixture of elastomer:curing agent was manually stirred for five minutes and poured onto the silicon master, contained within a small polystyrene weighing dish (Fisher). The sample was place under vacuum for 20 min in order to remove any air bubbles trapped during stirring. Curing was completed within 12 h through the use of a 65 W full spectrum incandescent bulb (GE). Stamps typically resulted in a total thickness of 8 mm. When called for, stamp surfaces were rendered hydrophilic through exposure to oxygen plasma by a facile 5 min exposure to a Tesla coil (Electro-Technic, Inc., model BD10A,

10,000-50,000 V, 500 kHz) at a tip distance of 2 cm, and stored in deionized water when not in use.

μ-CP on Ge. Approximately 1 mL of aqueous 2 x 10^{-3} M Na_2PdCl_4 was dropped onto the surface of the Ge wafer fragment. Immediately, the ozone-treated PDMS stamp was forced through the $PdCl_4^-$ solution with moderate pressure, so that direct contact with the underlying substrate was achieved. The PDMS stamp served as a barrier to "mask" the Ge surface from the aqueous metal solution, thereby preventing nanoparticle deposition in the regions where the stamp and substrate were in direct contact. After a period of 1 min, the excess metal solution was washed away with deionized water and the substrate transferred to a water bath while maintaining contact with the PDMS stamp. While immersed in deionized water, the stamp was removed and the substrate subsequently rinsed with additional water.

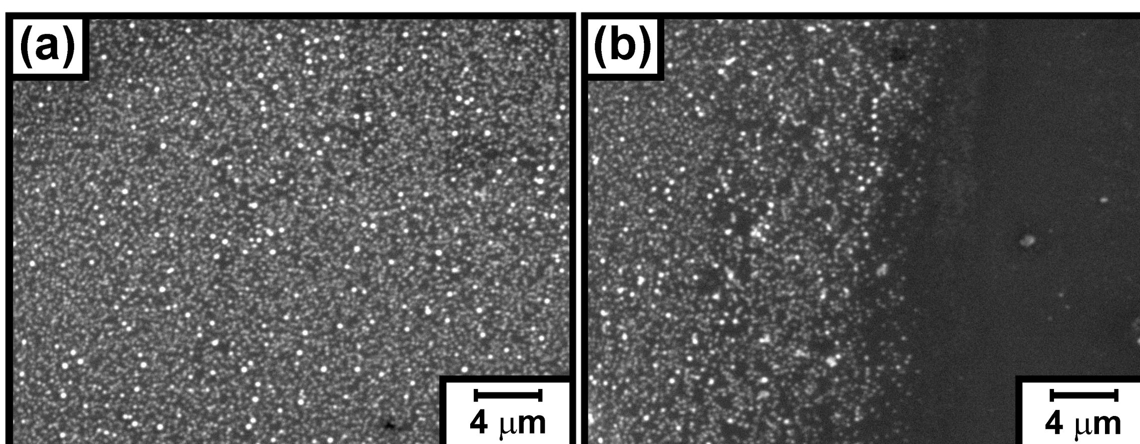

Figure SI-10. Scanning electron micrographs of μ-CP patterned deposition of Pd nanoparticles on a Ge(100) surface. The PDMS stamps served to force the metal salt solution clear from any areas in which the stamp makes firm contact with the underlying Ge substrate. The remaining areas, still exposed to the 2 mM Na_2PdCl_4 solution proceed to form a nanoparticle film (a). As long as the PDMS stamp features are clean and sharply formed, edges are well-defined (b).

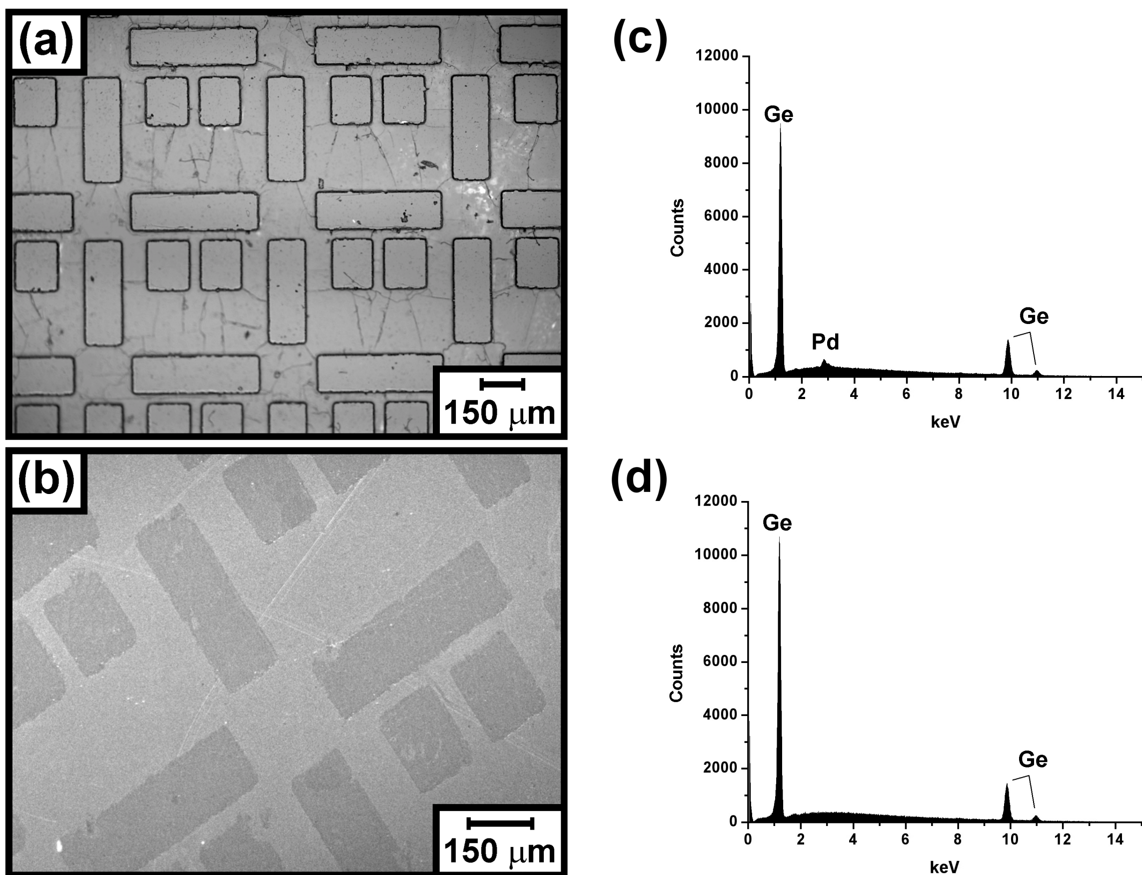

Figure SI-11. Optical micrograph (a) of the PDMS stamp used in negative patterning of Pd on Ge(100). Scanning electron micrographs of μ-CP deposition of Pd upon a Ge(100) surface (b). EDS confirms the deposition pattern, as observed by SEM. The EDS spectrum taken for the bright areas (c) confirms nanoparticles composed of Pd, whereas the Pd signal is absent from the EDS spectrum for the squares and rectangle regions (d).

μ-CP on Zn Foil. A freshly prepared PDMS stamp (not rendered hydrophilic with oxygen plasma) was soaked in deionized (18 MΩ·cm) water, was pressed upon a 2 x 10^{-2} M aqueous solution of $NaPtCl_4$ for 15-30 s. After drying the stamp at ambient conditions (30-50% relative humidity), both the stamp and a cut piece of Zn foil were stored in a humid (≥95%) jar for 5 min. The stamp was then lightly placed upon the foil for 15 s and removed; the foil was washed with deionized water and dried with dinitrogen flux.

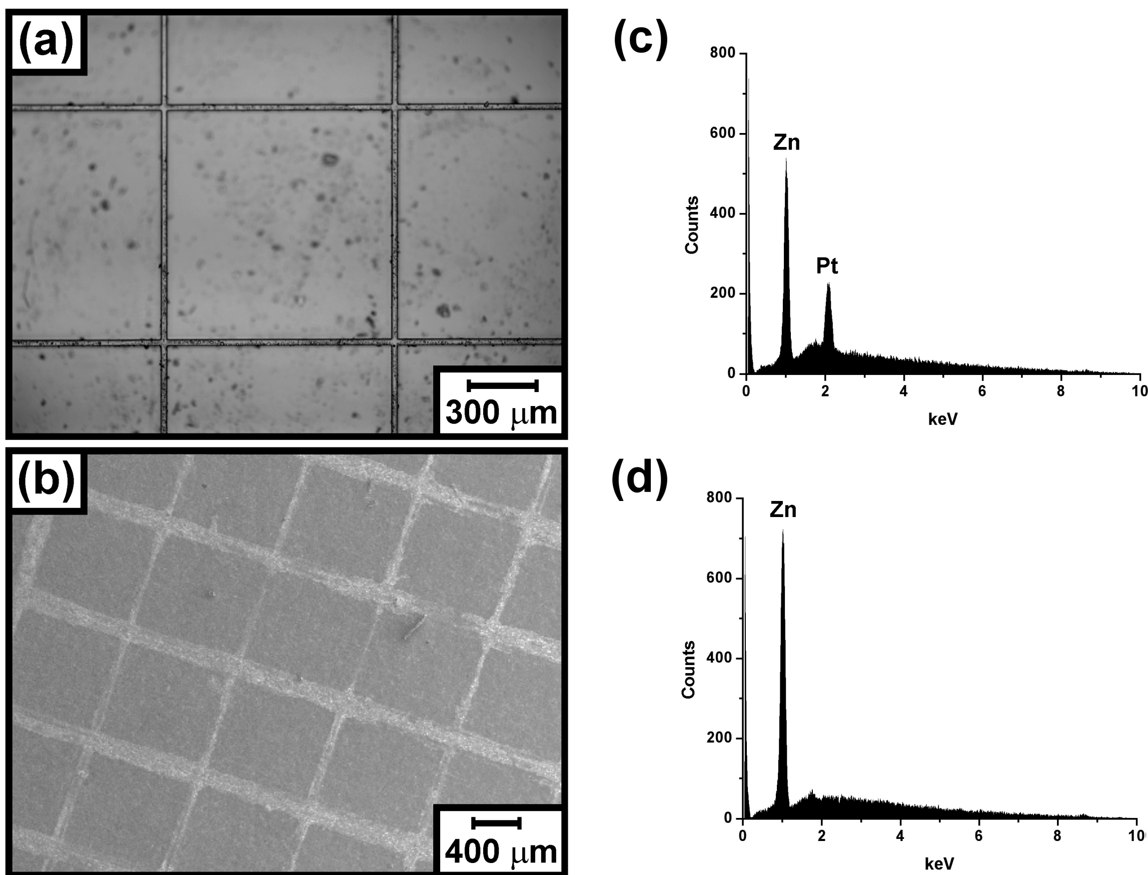

Figure SI-12. Optical micrograph (a) of the PDMS stamp used in negative patterning of Pt on Zn foil. A less complex PDMS stamp was utilized to compensate for the roughness of the metal foil, as compared to the flat Ge substrates used in the previous method. Scanning electron micrographs of μ-CP deposition of Pt upon a Zn foil surface (b). EDS confirms the deposition pattern, as observed by SEM. The EDS spectrum taken for the bright grid lines (c) confirms nanoparticles composed of Pt, whereas the Pt signal is absent from the EDS spectrum for the square regions (d).

Patterning Procedures: (iii) DPN

A scanning probe microscope (Nanoscope III, Digital Instruments) was used as a lithography tool for writing and tapping mode atomic force microscopy (TM-AFM) for imaging. The Si tip was dipped into an *ink* solution [1:10 (v:v) mixture of aqueous solution of 20 mM $AuCl_4^-$ and acetonitrile (99.8 %, Aldrich)] for 5 min and dried under ambient conditions for 5 min. The humidity during writing was held constant at 50 % using home-built humidifier. The writing speed for lithography was 0.2 μm/s for writing and 1.0 μm/s for imaging. The average height of the resulting gold line is about 4 nm and the diameter is in the range of 30 nm. While the height of a solid sample, such as gold, is usually accurate, the width of the observed line is widened due to convolution artifacts, a well-known issue in STM [R. Chicon, M. Ortuno and J. Abellan. *Surf Sci.* 181 107 (1987)] and AFM [J.S. Villarubbia, J. Res. Natl. Inst. Stand. Technol. 102, 425 (1997)], which causes the x,y-dimensions of sample features to appear larger as they are

in reality when their dimensions are in the range of the tip-curvature. In our case the same tip used for writing and imaging and is, therefore, due to wear and pollution, likely to result in a tip with enlarged curvature and decreased accuracy of the line diameter.